PRACE days 15: Enable Science Foster Industry   Dublin, Ireland 26-28 May 2015

NUMERICAL SIMULATION OF NON-PREMIXED SWIRLING FLAMES

Ruben PEREZ and Teresa PARRA

Dept. of Energy Engineering and Fluid Mechanics, University of Valladolid, Spain   terpar@eii.uva.es

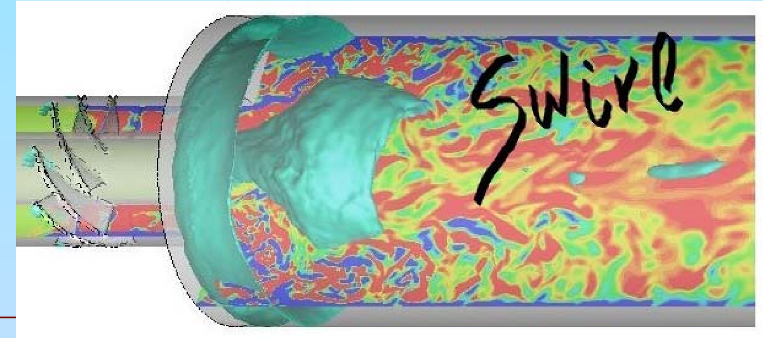

1 Physical model

	Roback & Johnson
R_{i1}	12.5 mm
R_{i2}	15.3 mm
R_a	29.5 mm
R_o	61.0 mm
S	50 mm
L	1 m

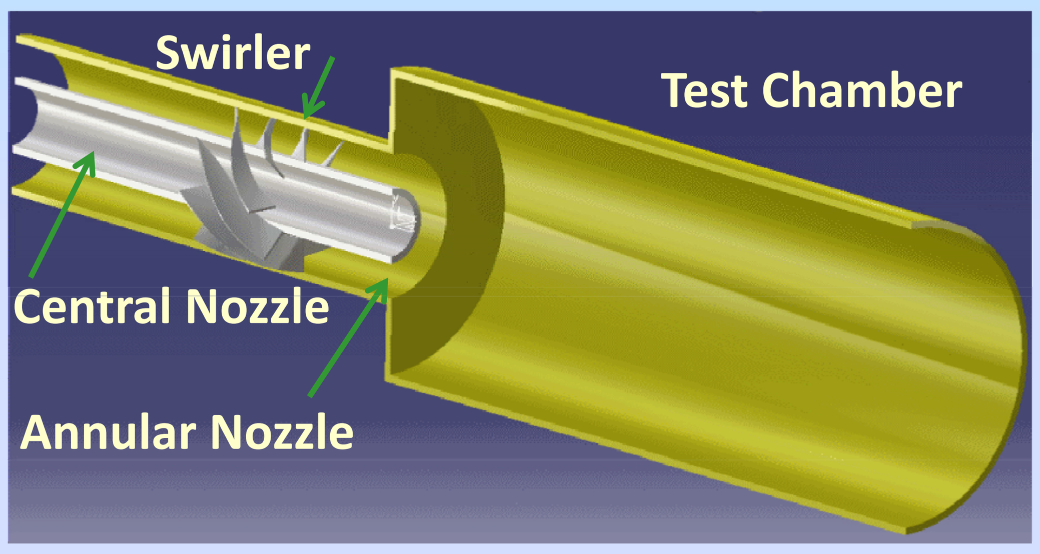

Ref. Roback R., Johnson B.V. (1983) Mass and momentum turbulent transport experiments with confined swirling coaxial jets, NASA CR-168252

2 Numerical Model

Geometry	3D
Mesh	Hexahedral 4 Million cells
Scheme	2nd order
P&V coupling	SIMPLE

		Fuel	Air
Inlet		Central nozzle	Annular nozzle
Composition	Stoichiometric mixture (λ=1)	19% CH_4+81%N_2	22% O2, 78% N2
	Lean mixture (λ=1.2)	16% CH_4+84%N_2	
	Lean mixture (λ=1.4)	14% CH_4+86%N_2	
Temperature (K)		300	900
Velocity (m/s)		0.66	1.54
Turbulence Intensity (%)		12	7.5
Density (kg/m³)		0.6679	1.225
Specific heat (J/kg/K)		Polynomial function of temperature	
Thermal conductivity (W/m/K)		0.0332	0.0242
Viscosity (kg/m/s)		1.087.10-5	1.7894.10-5
Molecular Weight (kg/kg/mol)			28.996

Thermally insulated chamber

Swirl number

$$S = \frac{\int \rho (r v_\theta) v_z 2\pi r dr}{R \int \rho v_z^2 2\pi r dr}$$

Swirl	0.14	0.74	0.95
Trailing Edge Angle	25º	54º	64º
Chord (m)	0.05	0.025	0.05

Axial Swirler is composed by 8 flat blades. Swirl number is modified by changing the trailing edge angle.

3 Turbulence Model

RNG K-Epsilon Turbulence Model for Swirl Dominated Flows

Turbulent Kinetic Energy transport equation

$$\frac{\partial}{\partial t}(\rho k) + \frac{\partial}{\partial x_i}(\rho k u_i) = \frac{\partial}{\partial x_j}\left(\alpha_k \mu_{eff}\frac{\partial k}{\partial x_j}\right) + G_k - \rho\varepsilon$$

Rate of Dissipation of Turbulent Kinetic Energy transport equation

$$\frac{\partial}{\partial t}(\rho\varepsilon) + \frac{\partial}{\partial x_i}(\rho\varepsilon u_i) = \frac{\partial}{\partial x_j}\left(\alpha_\varepsilon \mu_{eff}\frac{\partial \varepsilon}{\partial x_j}\right) + C_{1\varepsilon}\frac{\varepsilon}{k}G_k - C_{2\varepsilon}\rho\frac{\varepsilon^2}{k} - R_\varepsilon$$

Source term R_ε represents the rate of strain defined by

$$R_\varepsilon = \frac{C_\mu \eta^3 \rho (1-\eta/\eta_0)}{1+\beta\eta^3}\frac{\varepsilon^2}{k}$$

Cμ	C1ε	C2ε	η0	β
0.0845	1.42	1.68	4.38	0.012

$$\eta = (2 S_{ij} S_{ij})^{0.5} k/\varepsilon$$

4 Validation with experimental data for Swirl no. 1.0

Velocity profiles vs radial length for non reactive case

Axial Velocity | Azimuthal Velocity | Radial Velocity

Axial length 5 mm

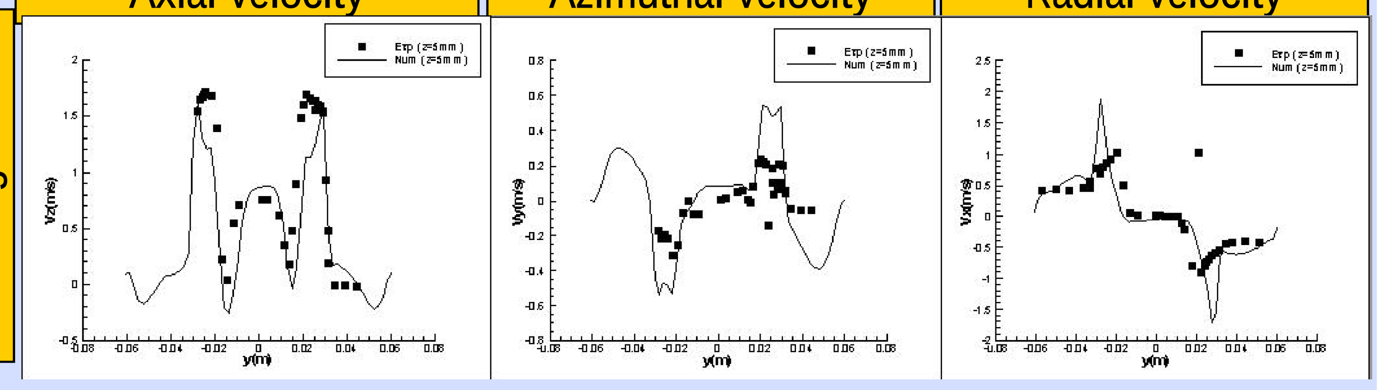

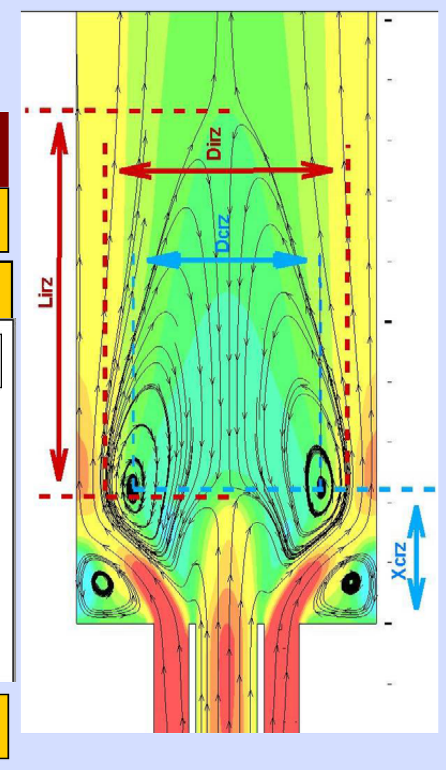

5 Combustion Model

Probability Density Function (PDF)

Mean Mixture Fraction transport equation

$$\frac{\partial}{\partial t}(\rho\bar{f}) + \frac{\partial}{\partial x_i}(\rho u_i \bar{f}) = \frac{\partial}{\partial x_i}\left(\frac{\mu_t}{\sigma_t}\frac{\partial}{\partial x_i}\bar{f}\right)$$

Mixture Fraction Variance transport equation

$$\frac{\partial}{\partial t}(\rho\overline{f'^2}) + \frac{\partial}{\partial x_i}(\rho u_i \overline{f'^2}) = -C_d \rho\frac{\varepsilon}{k}\overline{f'^2} + + \frac{\partial}{\partial x_i}\left(\frac{\mu_t}{\sigma_t}\frac{\partial}{\partial x_i}\overline{f'^2}\right) + C_g \mu_t\left(\frac{\partial}{\partial x_i}\bar{f}\right)^2$$

σ_t	C_g	C_d
0.7	2.86	2

Probability Density Function, p(f), let obtain local temperature from tabulated experimental results

$$\bar{T} = \int_0^1 p(f) T(f) df$$

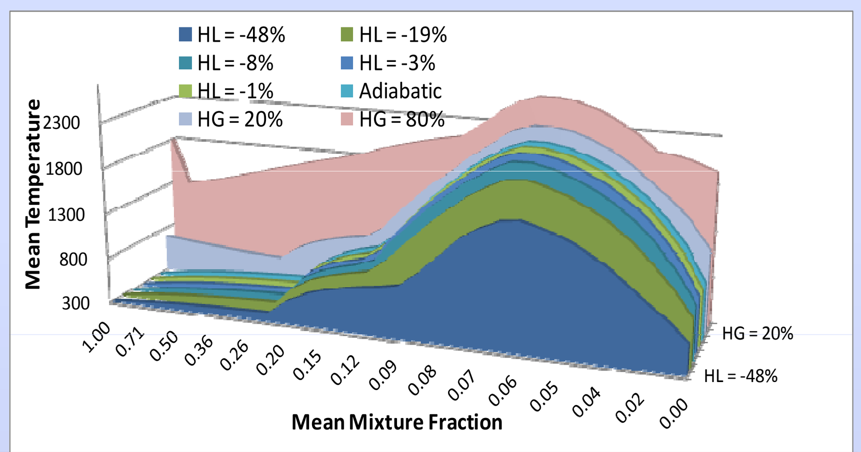

6 Influence of Swirl Number on Combustion

Scatter plots of temperature versus methane mass fraction

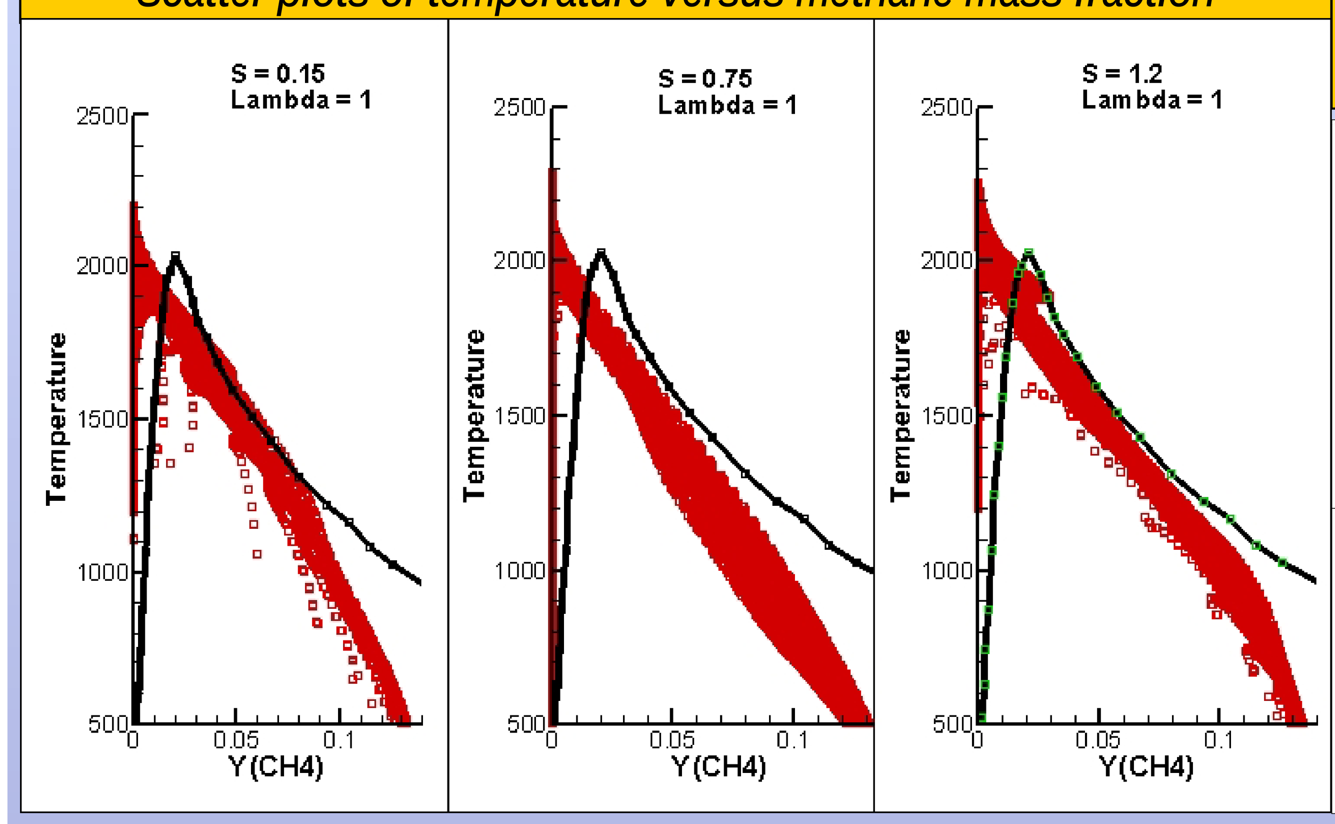

Contours of Mean Mixture Fraction and its Variance with surface of null axial velocity

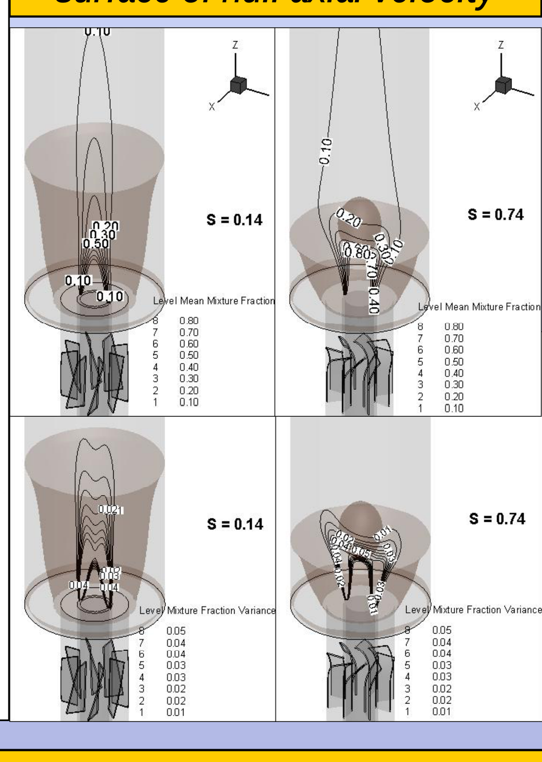

Surface of iso-temperature of 1400 and 1800 K from stoichiometric flames at different swirl numbers

Swirl no. 0.15 | Swirl no. 075 | Swirl no. 1.2

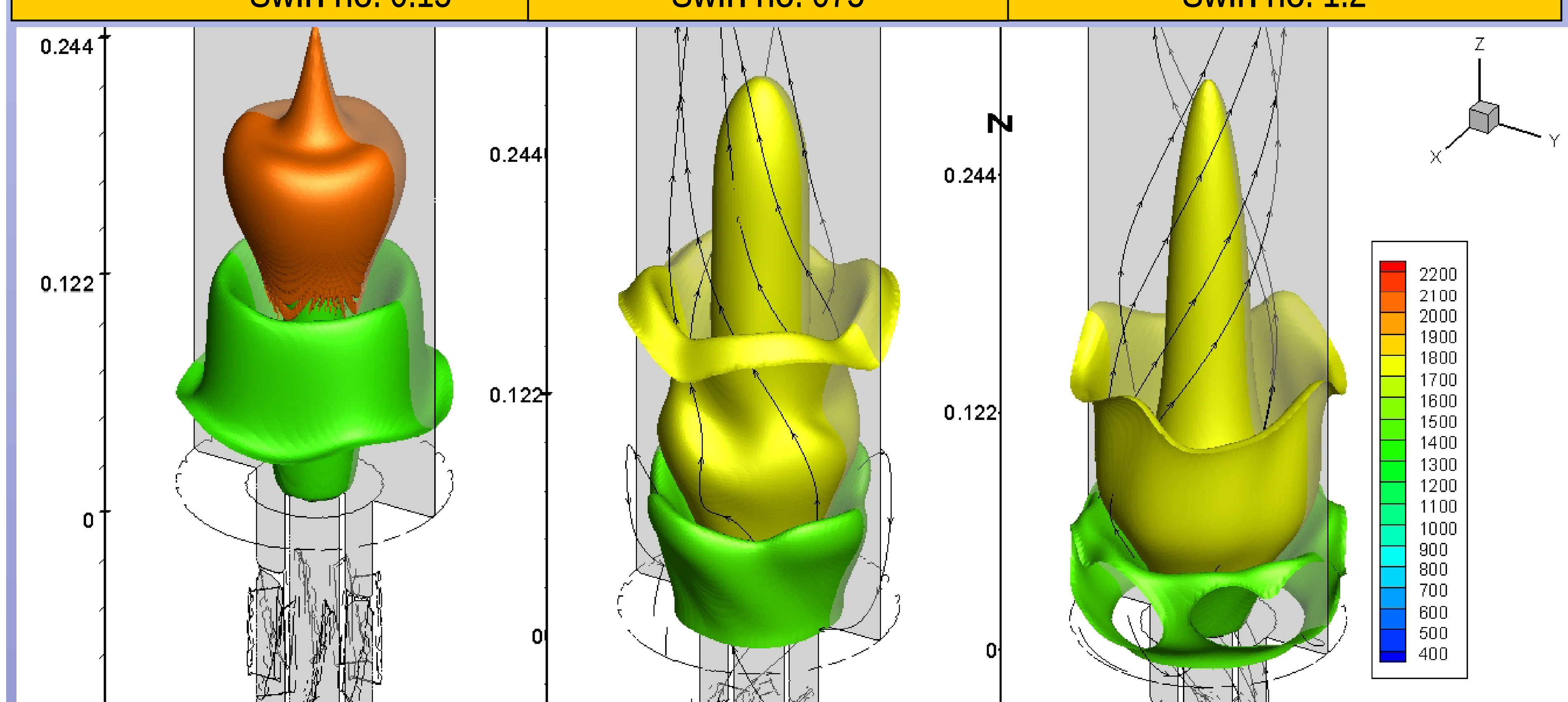

7 Influence of Stoichiometry

Contours of temperature and NO for stoichiometric and lean flames

Swirl no. 0.14 | Swirl no. 074

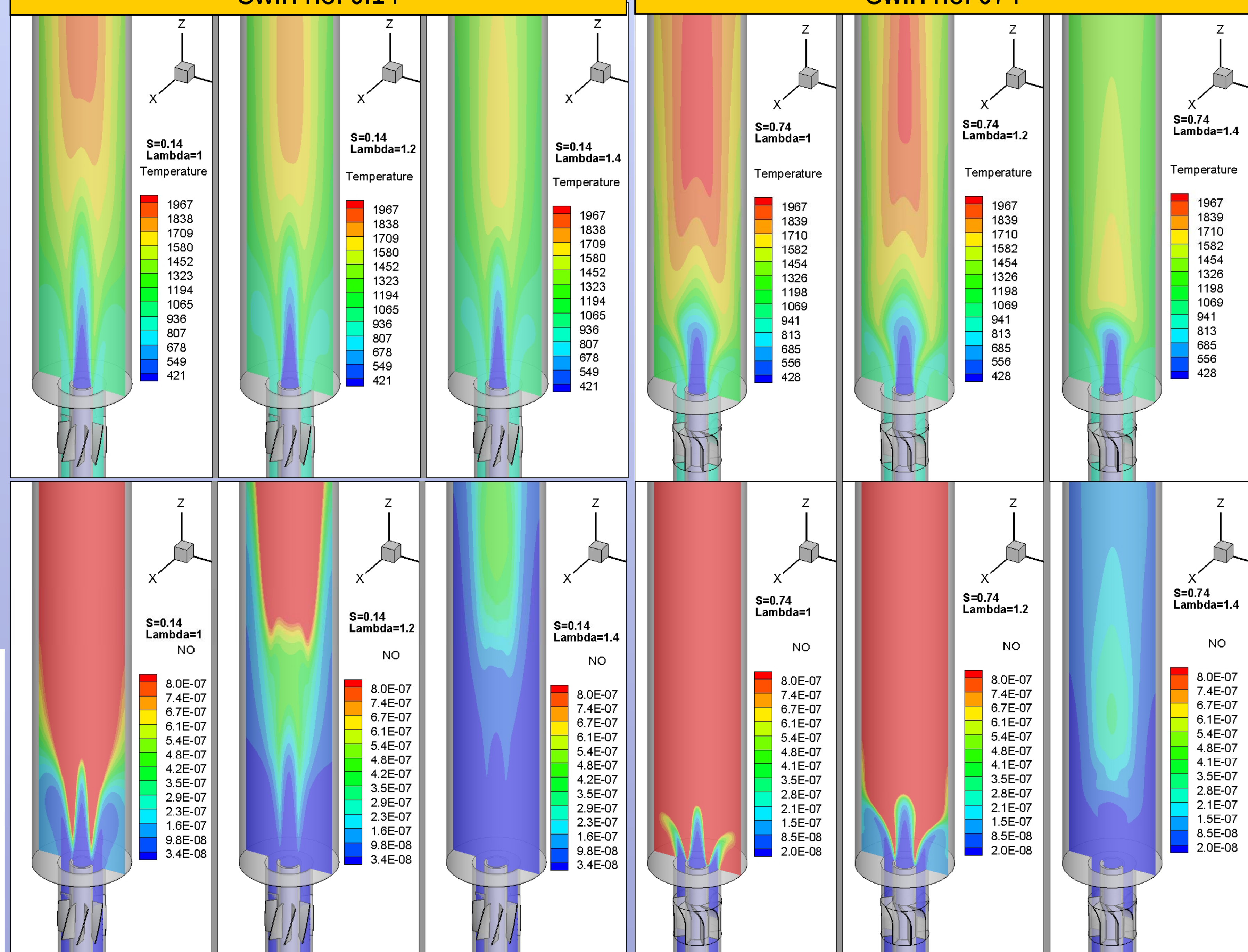

Conclusions

Low swirling injectors do not promote the fluid to turn over near the centre of the chamber, resulting larger mixing and reaction zones with weak gradients of temperature and species' mass fractions. Whereas, high swirl burners promote the formation of an inner recirculation zone with hot products of reaction. The lead stagnation point of the IRZ plays an important role fixing the location of the flame front in swirling burners.

At constant stoichiometry, high swirl burners promote thinner flame fronts, higher equilibrium temperature and higher nitrogen monoxide emissions than those of low swirl burners. These aspects offer a chance of using lean mixtures with the corresponding reduction of methane consume and NOx emissions.

Acknowledgment

The work has been developed in the framework of the project reference ENE2011-25468 from the Spanish Ministry of Science and Innovation. Authors acknowledge PRACE for awarding access to resources Curie-GENCI@CEA based in France and MareNostrum@BSC based in Spain. Ref. 2010PA1766. The Implementation Phase of PRACE receives funding from the EUs Seventh Framework Programme (FP7/2007-2013) under grant agreement RI-312763

REFERENCES: http://www.researcherid.com/rid/L-9473-2014
http://orcid.org/0000-0002-2274-3185

Universidad de Valladolid | ESCUELA de INGENIERÍAS INDUSTRIALES | GOBIERNO DE ESPAÑA | MINISTERIO DE CIENCIA E INNOVACIÓN | Barcelona Supercomputing Center, Centro Nacional de Supercomputación | GENCI